Accuracy of TLM Solutions of Maxwell's Equations

Leonardo R. A. X. de Menezes, *Member, IEEE,* and Wolfgang J. R. Hoefer, *Fellow, IEEE*

Abstract— **This work investigates the physical origin of the coarseness and dispersion errors influencing TLM solutions of Maxwell's equations. The study is performed by solving the difference equations of the numerical method analytically. The results confirm a reduction of the accuracy of the discrete solution near field singularities. This effect is a consequence of the finite number of spatial modes supported by the discretized domain. The solution of partially filled waveguide is also investigated. The results show that TLM can have positive or negative dispersion, depending on the dielectric filling, excited mode and the geometry. These results are also valid for the finite difference time domain method (FDTD).**

I. Introduction

In most cases, the solution of electromagnetic problems relies on the use of numerical methods [1]. Some of these techniques use the approximation of differential by difference operators [2]. This represents the substitution of the continuous problems by a discrete approximation. In all consistent numerical methods, the solution of these difference equations approaches the solution of the differential equations as the discretization step tends to zero, [3], [4].

The rate of convergence of the numerical solution characterizes the accuracy of the method. A numerical method is second-order accurate if the numerical solution approaches the continuous one with the square of the discretization step. The TLM and FDTD methods are second-order accurate methods. This result is obtained by a dispersion analysis of the scheme [5], [6].

This analysis is performed in homogeneous unbounded space [5]. In the presence of discontinuities a second-order accurate method can have different convergence rates. The discrete solution can converge slower to the continuous one in the presence of field singularities. The reason is the finite number of modes supported by the mesh that represents the continuous space.

In the characterization of the discontinuity, an infinite sum of modes describes the field behavior, [7]. However, in the discretized problem the number of supported modes is finite. The number of modes is related to the number of cells representing the domain. Therefore a finite sum of modes replaces the infinite one. This truncation is the cause of the coarseness error. In these cases, the convergence of the truncated sum of modes determines the convergence of the numerical method. If the series has first order convergence then that is also the case for the numerical method.

Another factor that affects the convergence behavior is the presence of more than one dielectric and magnetic material. In homogeneous problems the dispersion increases with the constitutive parameters of the modeled medium. However, this paper shows that this is not the case in inhomogeneous problems. In the case of the partially filled waveguide, the overall error did not increase monotonically with the volume of the dielectric filling. The result suggests that the main source of error in inhomogeneous space is not dispersion, but the representation of dielectric interface conditions in the discrete problem.

The dispersion analysis of the difference equation does not predict these effects. In this paper we advance in the characterization of numerical methods by solving analytically the difference equation of the numerical scheme. The equations are solved with the actual boundary conditions of the problem, using techniques suggested by Amari [8]. The closed form solution can only be obtained for certain cases. However, it allows to draw some conclusions about the propagation behavior of the modes present in the general case.

In TLM, closed form solutions can explain the behavior of the field near sources and discontinuities, their interaction with absorbing boundaries, and frequency shifts of results.

In this work, the analytical solution of the two-dimensional (2-D) shunt node TLM model is obtained for some examples. Two of these examples, the capacitive diaphragm in a TEM waveguide and the partially filled waveguide, [7], present results that cannot be explained by dispersion analysis. The behavior of the diaphragm susceptance in the discrete TEM waveguide shows a reduction of the convergence rate of the method. The solution of the partially filled waveguide shows that the main source of error in inhomogeneous problems is not the dispersion, but the implementation of the interface conditions.

II. Theory

The analytical solution of the discrete problem, subject to boundary and initial conditions, characterizes completely the behavior of the numerical method. The solution of these equations is similar to the continuous problem. The partial difference equation is reduced to a set of one-dimensional (1-D) difference equations using separation of variables.

Once the set of 1-D difference equations is obtained, the z-transform technique or a finite Fourier series is used to obtain

Manuscript received March 29, 1996. This work was supported in part by the Brazilian government agency CNPq.

The authors are with NSERC/MPR Teltech Research Chair in RF Engineering. Department of Electrical and Computer Engineering, University of Victoria, Victoria B.C., Canada.

Publisher Item Identifier S 0018-9480(96)08560-2.

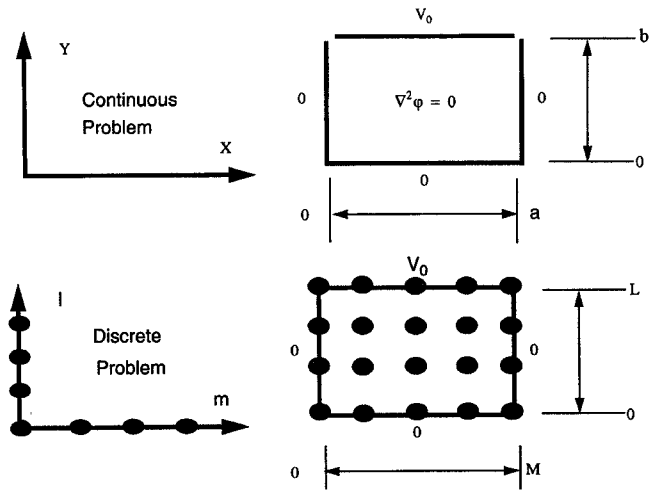

Fig. 1. The potential box problem. The solutions are obtained by solving the continuous and discrete Laplace equations.

the solution of the problem subject to the boundary conditions. The following example illustrates the general solution procedure.

Consider the two-dimensional Laplace equation in a potential box, Fig. 1 [9]. The Laplace equation describes the continuous problem

$$\nabla^2\phi = 0 \tag{1}$$

subject to the boundary conditions

$$\varphi(0, y) = 0 \qquad \varphi(a, y) = 0 \qquad \varphi(x, 0) = 0$$

$$\varphi(x, b) = V_0. \tag{2}$$

The analytical solution is

$$\varphi(x, y) = \frac{4V_o}{\pi} \sum_{n=1,3}^{\infty} \frac{1}{n} \frac{\sin\left(n\frac{\pi}{a}x\right) \sinh\left(n\frac{\pi}{a}y\right)}{\sinh\left(n\pi\frac{b}{a}\right)}. \tag{3}$$

Consider now the discrete equivalent of the potential box (Fig. 1), characterized by the five-point finite difference (FD) scheme [10]

$$\varphi(m, l) = \frac{1}{4}(\varphi(m+1, l) + \varphi(m-1, l) + \varphi(m, l+1) + \varphi(m, l-1)). \tag{4}$$

The boundary conditions of the continuous case are also applied to the discrete problem. The box is discretized into a rectangular mesh of M by L points. The discretization step Δs is such that

$$a = M\Delta s$$
$$b = L\Delta s. \tag{5}$$

The five-point difference scheme (4) can be rewritten as

$$\frac{\varphi(m+1, l) - 2\varphi(m, l) + \varphi(m-1, l)}{\Delta s} + \frac{\varphi(m, l+1) - 2\varphi(m, l) + \varphi(m, l-1)}{\Delta s} = 0. \tag{6}$$

This equation represents the sampling of a continuous field over a domain, in discrete points. Since the field is defined at each sampling point, the separation of variables is possible at these points

$$\varphi(m, l) = X(m)Y(l). \tag{7}$$

Substituting the solution (7) into (6) result in

$$\frac{X(m+1) - 2X(m) + X(m-1)}{X(m)} + \frac{Y(l+1) - 2Y(l) + Y(l-1)}{Y(l)} = 0 \tag{8}$$

which can be expressed as two 1-D equations

$$X(m+1) = (2 - k_x^2)X(m) - X(m-1)$$

$$Y(l+1) = (2 - k_y^2)Y(l) - Y(l-1) \tag{9}$$

with the dispersion relationship

$$k_x^2 + k_y^2 = 0. \tag{10}$$

The solutions of (9) are of the form

$$X(m) = A_1\, exp\,(-j\alpha m) + A_2\, exp\,(j\alpha m)$$

$$Y(l) = B_1\, exp\,(-j\beta l) + B_2\, exp\,(j\beta l). \tag{11}$$

The solution in the m-direction is obtained by applying the boundary conditions of the discrete problem, together with the dispersion relation

$$\varphi(0, l) = 0$$
$$\varphi(M, l) = 0 \tag{12}$$

resulting in the function

$$X(m) = A\sin\left(\frac{n\pi}{M}m\right) \qquad k_x = 2\sin\left(\frac{n\pi}{2M}\right). \tag{13}$$

The solution in the l direction is obtained by applying the boundary condition in the l direction

$$\varphi(m, 0) = 0. \tag{14}$$

The solution in the l direction is

$$Y(l) = B\sin(\beta l) \qquad \beta = 2\sin^{-1}\left(\frac{k_y}{2}\right). \tag{15}$$

Using the dispersion relationship

$$k_z = 2j\sin\left(\frac{n\pi}{2M}\right) \tag{16}$$

results in the solution

$$X(m) = A\sin\left(\frac{n\pi}{M}m\right)$$
$$Y(l) = B\sinh\left(2l\sinh^{-1}\left(\sin\left(\frac{n\pi}{2M}\right)\right)\right). \tag{17}$$

Using the remaining boundary condition

$$\varphi(m, L) = V_0. \tag{18}$$

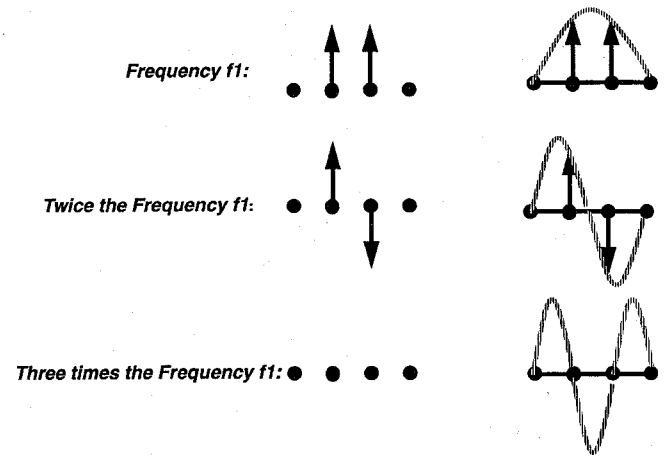

Fig. 2. Number of modes in a discrete structure. The number of allowed modes is equal to the number of free nodes. The natural consequence is that any infinite sum of modes is truncated to the number of free nodes in the discrete problem.

The solution in the m direction involves the use of a finite Fourier series in the form

$$\sum_{n=0}^{M-1} a_n \sin\left(\frac{n\pi}{M}m\right) \sinh\left(2L\sinh^{-1}\left(\sin\left(\frac{n\pi}{2M}\right)\right)\right) = V_0. \tag{19}$$

The Fourier sum (instead of integral) is used to obtain the coefficients of the series

$$\sum_{k=0}^{M-1}\left[\sum_{n=0}^{M-1} a_n \sin\left(\frac{n\pi}{M}m\right) \sinh\left(2L\sinh^{-1}\left(\sin\left(\frac{n\pi}{2M}\right)\right)\right)\right] \cdot \sin\left(\frac{\pi k}{M}m\right) = \sum_{k=0}^{M-1} V_0 \sin\left(\frac{\pi k}{M}m\right). \tag{20}$$

The coefficients of the series are

$$a_n = \frac{V_0(\cos(n\pi)-1)\sin\left(\frac{n\pi}{M}\right)}{M\left(\cos\left(\frac{n\pi}{M}\right)-1\right)\sinh\left(2L\sinh^{-1}\left(\sin\left(\frac{n\pi}{2M}\right)\right)\right)} \tag{21}$$

which result in the solution

$$\varphi(m,\, l) = \sum_{n=1,\,3}^{M-1}\left[\frac{2V_o}{M\sin\left(\frac{n\pi}{2M}\right)}\right] \cdot \frac{\sin\left(n\frac{\pi}{M}m\right)\sinh\left(2l\sinh^{-1}\left(\sin\left(\frac{n\pi}{2M}\right)\right)\right)}{\sinh\left(2L\sinh^{-1}\left(\sin\left(\frac{n\pi}{2M}\right)\right)\right)}. \tag{22}$$

The comparison between (3) and (22) shows an interesting relationship between the modes of the continuous and the discrete cases. There is a perfect correspondence between the mathematical expressions, but not between the number of modes. While the continuous problem involves an infinite number of modes, the discrete problem involves a finite set. In the numerical scheme, there are only as many modes as there are free points in the mesh. These points do not lie in the boundary. This can be visualized in Fig. 2. The importance of (22) resides in the truncation of the series represented in (3). The convergence of the method is connected not only to the dispersion relationship, but also to the series of modes. If the series has only first order convergence so does the solution.

TABLE I
RESULTS FOR THE POTENTIAL BOX. THE TABLE SHOWS THE CALCULATED AND SIMULATED POTENTIAL AT SELECTED POINTS INSIDE THE RECTANGULAR BOX. EACH POINT IS DETERMINED BY THE (X, Y) COORDINATES

X,Y point	ϕ analytical	ϕ numerical	ϕ discrete
(a/4,b/4)	6.7972	7.14286	7.14285713
(a/4,b/2)	18.2028	18.75000	18.74999999
(a/4,3b/4)	43.2028	42.85714	42.85714281

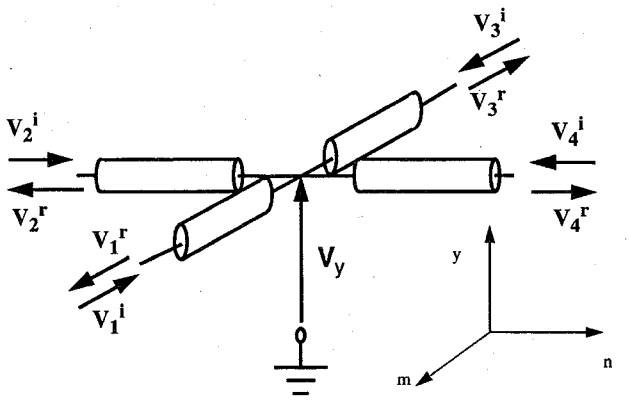

Fig. 3. Two-dimensional shunt node.

A comparison between the results obtained with (3), (22) and the numerical implementation of (4) (with $V_0 = 100$ V, $M = L = 5$) is shown in Table I. The difference between the numerical implementation of (4) and its analytical solution (22) is due only to the round-off error.

The analytical solution of the finite difference scheme is very useful in the case of TEM structures. Some of the static TLM solutions are also obtained by solving the five-point scheme presented in (4). In the case of complex problems, a more detailed analysis of the method is necessary.

In the case of TLM, the scattering and propagation of voltages represent the difference equations that describe the electric and magnetic fields. The procedure relies on the transmission line analogy, describing the propagation and scattering of voltage pulses through an array of transmission lines. During a simulation, the field components can be obtained from the stream of voltages pulses.

In the following analysis only 2-D TLM is considered. The analysis for the three-dimensional (3-D) case can be done in a similar way with the use of electric and magnetic potentials.

Consider the 2-D TLM shunt node shown in Fig. 3, [1].

For each node, the scattered voltages are obtained from the incident voltages by

$$\begin{bmatrix}\nu_1\\ \nu_2\\ \nu_3\\ \nu_4\end{bmatrix}^r_{k+1} = \frac{1}{2}\begin{bmatrix}-1 & 1 & 1 & 1\\ 1 & -1 & 1 & 1\\ 1 & 1 & -1 & 1\\ 1 & 1 & 1 & -1\end{bmatrix}\begin{bmatrix}\nu_1\\ \nu_2\\ \nu_3\\ \nu_4\end{bmatrix}^i_k \tag{23}$$

and the n transferred to neighboring nodes by

$$\nu_1^i(m,\, n) = \nu_3^r(m+1,\, n) \qquad \nu_4^i(m,\, n) = \nu_2^r(n+1)$$
$$\nu_3^i(m,\, n) = \nu_3^r(m-1,\, n) \qquad \nu_2^i(m,\, n) = \nu_4^r(n-1). \tag{24}$$

The field components are obtained using the mapping

$$\begin{bmatrix} E_y \\ Z_0 H_x \\ Z_0 H_z \end{bmatrix} = \frac{1}{2}\begin{bmatrix} 1 & 1 & 1 & 1 \\ \sqrt{2} & 0 & -\sqrt{2} & 0 \\ 0 & -\sqrt{2} & 0 & \sqrt{2} \end{bmatrix}\begin{bmatrix} \nu_1 \\ \nu_2 \\ \nu_3 \\ \nu_4 \end{bmatrix}^i. \quad (25)$$

There is not a unique mapping from three-field components to four-voltage pulses. Considering the fourth eigenvector solution of the dispersion relationship as an additional field component W results in a unique mapping. The component obtained from the null space of (25) has the dimensions of an electric field. The mapping is

$$\begin{bmatrix} \nu_1 \\ \nu_2 \\ \nu_3 \\ \nu_4 \end{bmatrix}^i = \frac{1}{2}\begin{bmatrix} 1 & \sqrt{2} & 0 & 1 \\ 1 & 0 & -\sqrt{2} & -1 \\ 1 & -\sqrt{2} & 0 & -1 \\ 1 & 0 & \sqrt{2} & 1 \end{bmatrix}\begin{bmatrix} E_y \\ Z_0 H_x \\ Z_0 H_z \\ W \end{bmatrix}. \quad (26)$$

The additional field component completes the bijective mapping between field components and voltages.

Using this mapping (26), the TLM algorithm is transformed into a set of field difference equations. The electric field difference equation is

$$\begin{aligned} E_y^{k+1}(m, n) = \frac{1}{2}[&E_y^k(m+1, n) + E_y^k(m-1, n) \\ &+ E_y^k(m, n+1) + E_y^k(m, n-1)] \\ &- E_y^{k-1}(m, n). \end{aligned} \quad (27)$$

And the remaining components

$$\begin{aligned} H_x^{k+1}(m, n) &= H_x^k(m+1, n) + H_x^k(m-1, n) - H_x^{k-1}(m, n) \\ &+ \frac{1}{2Z_0}[W^k(m+1, n) - W^k(m-1, n)] \end{aligned}$$

$$\begin{aligned} H_z^{k+1}(m, n) &= H_z^k(m, n+1) + H_z^k(m, n-1) - H_z^{k-1}(m, n) \\ &+ \frac{1}{2Z_0}[W^k(m, n-1) - W^k(m, m+1)] \end{aligned}$$

$$W^{k+1}(m, n) = A^k + B^k - W^{k-1}(m, n)$$

$$\begin{aligned} A^k = \frac{1}{2}[&W^k(m, n+1) + W^k(m, n-1) \\ &- W_y^k(m+1, n) - W_y^k(m-1, n)] \end{aligned}$$

$$\begin{aligned} B^k = Z_0(&H_z^k(m, n+1) - H_z^k(m, n-1) \\ &- H_x^k(m+1, n) + H_x^k(m-1, n)). \end{aligned} \quad (28)$$

The electric field difference equation is independent from the remaining equations. Therefore it can be used to describe the evolution of all field components.

Once the electric field is determined, the magnetic field is obtained using

$$\begin{aligned} H_x^{k+1}(m, n) &= \frac{1}{4Z_0}[E_y^k(m+1, n) - E_y^k(m-1, n)] \\ H_z^{k+1}(m, n) &= \frac{1}{4Z_0}[E_y^k(m, n+1) - E_y^k(m, n-1)] \end{aligned} \quad (29)$$

and the additional field W is described by

$$\begin{aligned} W^{k+1}(m, n) = \frac{1}{4}[&E_y^k(m, n+1) + E_y^k(m, n-1) \\ &- E_y^k(m+1, n) - E_y^k(m-1, n)]. \end{aligned} \quad (30)$$

This independence of the electric field allows the solution of most problems by solving only one partial difference equation. The equation is solved using the boundary and initial conditions for the electric field. This is also the case in FDTD. In a 2-D problem, the results obtained with TLM and FDTD must be equal provided that both have the same field initial conditions (only $Ey(t = 0)$ is non-zero), discretization, and timestep. In the case of the series node, the magnetic field difference equation can be used to solve the TLM problem. This equation can be obtained in a procedure similar to the shunt case.

In another example, the electric field difference equation will be used to obtain the first cutoff wavenumber of a rectangular waveguide (width a and height b). In this case, the same results can be obtained also from the dispersion relationship [5]. However, this is a valuable example of the solution procedure. The analysis is simplified by considering sinusoidal excitation of the cavity.

The boundary conditions are

$$\begin{aligned} E_y^k(0, n) &= 0 \\ E_y^k(M, n) &= 0 \end{aligned} \quad (31)$$

$$\begin{aligned} E_y^k(m, 1) &= E_y^k(m, -1) \\ E_y^k(m, N-1) &= E_y^k(m, N+1) \end{aligned} \quad (32)$$

with the initial condition

$$E_y^k(m, n) = \delta(m - m_1)\delta(n - n_1)e^{j\omega_c \Delta t k} \quad (33)$$

where ω_c is the frequency of the resonant mode.

The field is described by

$$E_y^k(m, n) = X(m)Z(n)T(k). \quad (34)$$

Using separation of variables in the electric field equation results in the set of (1-D) equations

$$\begin{aligned} X(m+1) &= (2 - k_x^2)X(m) - X(m-1) \\ Z(n+1) &= (2 - k_z^2)Z(n) - Z(n-1) \\ T(k+1) &= (2 - k_0^2)T(k) - T(k-1). \end{aligned} \quad (35)$$

With the separation condition

$$2k_0^2 = k_x^2 + k_z^2. \quad (36)$$

Assuming that the solution is of the same form as (11), and using the boundary conditions in the 1-D equations

$$X(m) = A\sin\left(p\frac{\pi}{M}m\right) \qquad Z(n) = B\cos\left(q\frac{\pi}{N}n\right)$$

$$T(k) = e^{-j\omega_c \Delta t k} \quad (37)$$

TABLE II
RESULTS FOR THE RECTANGULAR WAVEGUIDE. THE TABLE SHOWS THE CALCULATED (USING DIFFERENCE EQUATIONS) AND SIMULATED NORMALIZED CUTOFF WAVENUMBER

Discretization (N)	ϕ analytical (k_0a)	ϕ numerical (k_0a)	ϕ discrete (k_0a)
N=10	3.1416	3.135	3.1351
N=20	3.1416	3.138	3.1401
N=40	3.1416	3.139	3.1412

with the relations

$$k_x = 2\sin\left(\frac{p\pi}{2M}\right) \qquad k_z = 2\sin\left(\frac{q\pi}{2N}\right)$$

$$k_0 = 2\sin\left(\frac{\omega_c \Delta t}{2}\right) \tag{38}$$

the cutoff frequencies are obtained by substituting (38) into (36), which yields the dispersion relationship of 2-D TLM

$$2\sin^2\left(\frac{\omega_c\Delta t}{2}\right) = \sin^2\left(\frac{p\pi}{2M}\right) + \sin^2\left(\frac{q\pi}{2N}\right). \tag{39}$$

The field is described by a series of modes in a cavity and by the Fourier transform of the time response

$$E_y^k(m,n) = \frac{1}{NM}\sum_{p=1}^{M-1}\sum_{q=1}^{N-1}\sin\left(\frac{p\pi}{M}m_1\right)\sin\left(\frac{q\pi}{N}n_1\right) \cdot \cos\left(\frac{p\pi}{M}m\right)\cos\left(\frac{q\pi}{N}n\right)e^{-j\omega_c\Delta t k}. \tag{40}$$

The other field components are obtained from (29) and (30). The resonant frequency ω_c is obtained by solving (39) for each resonant mode ($p = 1\cdots M-1$ and $q = 1\cdots N-1$).

This is a basic procedure for the solution of the difference equation. The results are shown in Table II for the dominant mode in a waveguide and compared to analytical results and simulations. In the next section, the electric field difference equation is used for two case examples. The results obtained in these cases cannot be explained by dispersion analysis.

III. RESULTS

The solution of the electric field partial difference equation was obtained for two particular examples. The first example is the calculation of the eigenvalues of a partially dielectric-filled 2-D cavity, [7]. The eigenvalues are compared to the exact values and the values obtained with TLM. The second example is the calculation of the susceptance of a capacitive diaphragm in a TEM waveguide, [7].

The partially filled cavity is shown in Fig. 4. The calculated eigenvalues for the first mode were obtained by subdividing the cavity in two homogeneous regions, and by enforcing the continuity of the field at the dielectric interface. The resulting transcendental equation was used to obtain the analytical

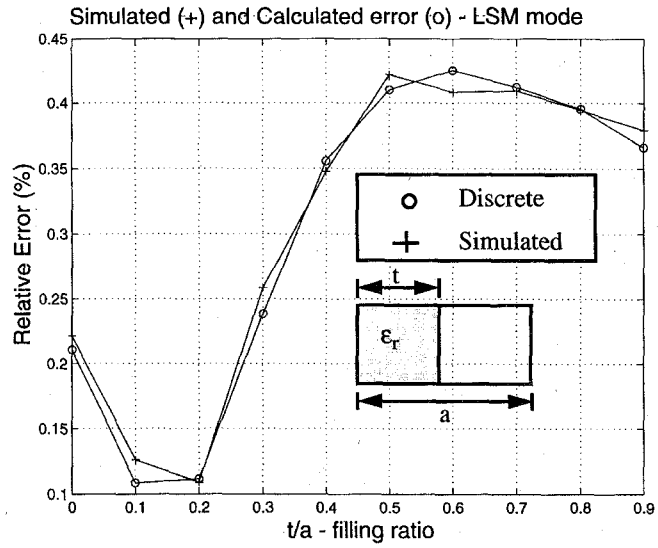

Fig. 4. Relative error of the first eigenvalue of the partially filled waveguide.

eigenvalues of the discrete problem

$$A + B = 0$$

$$A = \sin\left(2\,\mathrm{asin}\left[\sqrt{2\epsilon_r}\sin\left(\frac{\beta a}{2N\sqrt{2}}\right)\right]\right) \cdot \tan\left(2N\frac{t}{a}\,\mathrm{asin}\left[\sqrt{2\epsilon_r}\sin\left(\frac{\beta a}{2N\sqrt{2}}\right)\right]\right)$$

$$B = \epsilon_r \sin\left(2\,\mathrm{asin}\left[\sqrt{2}\sin\left(\frac{\beta a}{2N\sqrt{2}}\right)\right]\right) \cdot \tan\left(2N\left(1-\frac{t}{a}\right)\mathrm{asin}\left[\sqrt{2}\sin\left(\frac{\beta a}{2N\sqrt{2}}\right)\right]\right). \tag{41}$$

In the continuous case, the eigenvalues are calculated using

$$\beta a\sqrt{\epsilon_r}\tan\left(\beta a\sqrt{\epsilon_r}\frac{t}{a}\right) + \epsilon_r\beta a\tan\left(\beta a\left(1-\frac{t}{a}\right)\right) = 0. \tag{42}$$

The comparison between results for a ten-point discretization is shown in Fig. 4. This result shows that the main source of discrepancy between the continuous and discrete results is not the dispersion. If dispersion was the major source of error in the problem, the error would only increase with the filling ratio. The most likely cause is a surface effect in the interface between air and dielectric. The error tends to decrease with small dielectric fillings and increase with large ones, but not monotonically.

This result is confirmed by TLM simulations of the cavity. The reduction of the error cannot be explained only by dispersion analysis. Additional simulations show that the resonant frequencies may have positive shift with certain dielectric fillings or higher modes.

Therefore, TLM does not have only negative frequency shifts in inhomogeneous problems. This is only the case for homogeneous media. If two or more dielectrics are present in the simulation, the frequency shift may be positive or negative.

The second example was the solution of the electric field wave difference equation for the capacitive diaphragm in a

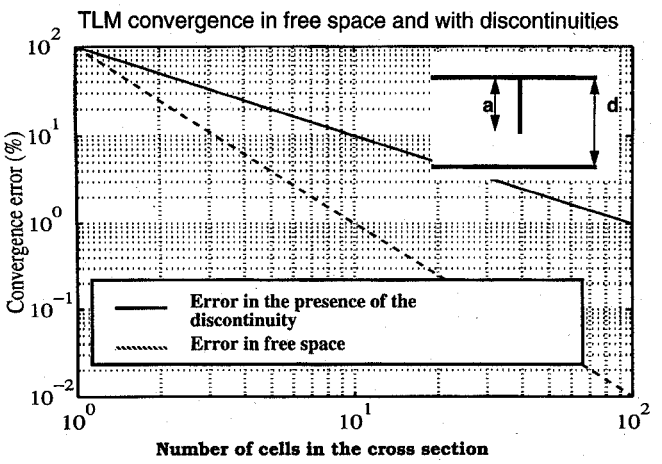

Fig. 5. Convergence of the error in the capacitive diaphragm and free-space cases.

TEM waveguide, resulting in the susceptance of the diaphragm in the discrete case. The results obtained by TLM (or FDTD) simulations are shifted in frequency. This shift was usually attributed to the coarseness error or to spurious modes localized at the discontinuity.

The solution of the discrete problem proves that the frequency shifts observed in several TLM simulations are not caused by spurious modes. The reason for the shift is the finite number of modes in the solution of the difference equation (the finite number of modes are the cause of the coarseness error of TLM meshes). However, due to the complexity involved in the solution of the difference equation for this problem, a closed form result for all frequencies is very difficult to obtain. In spite of this, the low frequency (static) solution can be obtained with the convergence bounds.

The summation of an infinite number of modes yields the analytical low frequency solution in the continuous case [7]

$$B_{exact} = \frac{4k_0 a}{\pi} ln\left[\sin\frac{\pi d}{2a}\right]. \tag{43}$$

The numerical solution is obtained with a finite sum of modes [10]. The result is bounded by

$$B_{exact} - \alpha\frac{4k_0\Delta x}{\pi} \leq B_{discrete} \leq B_{exact} + \alpha\frac{4k_0\Delta x}{\pi} \tag{44}$$

where α is a function of the aperture d/a.

These results show that the discrete solution has a different convergence behavior (from quadratic to linear) in the presence of certain discontinuities (infinitely thin walls). The reason, which is valid for logarithmic discontinuities, is the slow convergence of the mode series. Fig. 5 shows the convergence error of the method versus the number of cells. The rate of convergence of the susceptance is dependent on the number of modes near the discontinuity. The number of cells determines the number of modes allowed by the TLM difference equation. Therefore, the frequency shift, observed in TLM simulations of this type of discontinuity, is a natural result of the difference equation and not of spurious modes. The result can be improved by local modifications in the TLM mesh that include the static field behavior near the edge. The total effect is the improvement on the convergence of the series.

This kind of convergence behavior determines the coarseness error of the mesh. Therefore, in most real cases, the coarseness error is the dominant source of error in TLM simulations.

IV. Conclusion

This paper has presented the explanation for the frequency shifts observed in TLM simulations of structures with infinitesimally thin discontinuities. The reason is the reduction of the convergence rate of the method. The finite number of modes supported by the mesh causes this effect.

The first-order convergence of the TLM method with infinitesimally thin walls explains the frequency shifts observed in some simulations. The first-order term of the susceptance (44) appears as a stray capacitance in the problems. Therefore the calculated results shift down or up in frequency. The direction of the shift depends on whether the boundary is represented between or at the nodes. The frequency shift is a natural feature of the discrete scheme. It is not caused by the fourth eigenvector of the TLM method. These results are also valid for other second-order finite difference schemes.

This work has also shown an interface effect in the representation of inhomogeneous structures. The effect can be the main source of error in these cases. In the calculated example, the effect caused a reduction of the error in the case of small dielectric fillings. Additional analysis suggests that negative frequency shifts may be present in inhomogeneous structures. The effect is dependent in the mode configuration and position of the dielectric boundary. Therefore, positive frequency shifts can be present in two-dimensional TLM and FDTD simulations.

Acknowledgment

The authors would like to thank the helpful discussions and suggestions of Dr. S. Amari. The authors also thank the suggestions and comments provided by the reviewers of the paper.

References

[1] W. J. R. Hoefer, "The transmission line matrix method—theory and applications," *IEEE Trans. Microwave Theory Tech.*, vol. 33, pp. 882–893, Oct. 1985.
[2] G. D. Smith, *Numerical Solution of Partial Differential Equations*, 2nd ed. New York: Claredon Press, 1978.
[3] A. Ralston, *A First Course in Numerical Analysis.* New York: McGraw-Hill, 1965.
[4] J. Noye, Ed., *Computational Techniques for Differential Equations.* New York: North-Holland, 1984.
[5] J. S. Nielsen and W. J. R. Hoefer, "Generalized dispersion analysis and spurious modes of 2-D and 3-D TLM formulations," *IEEE Trans. Microwave Theory Tech.*, vol. 41, pp. 1375–1384, Aug. 1993.
[6] M. Krumpholz and P. Russer, "On the dispersion of TLM and FDTD," *IEEE Trans. Microwave Theory Tech.*, vol. 42, pp. 1275–1279, July 1994.
[7] R. E. Collin, *Field Theory of Guided Waves*, 2nd ed. New York: IEEE Press, 1991.
[8] S. Amari, Private Communication, Univ. of Victoria, 1995.
[9] D. T. Paris and F. K. Hurd, *Basic Electromagnetic Theory.* New York: McGraw-Hill, 1969.
[10] M. Abramowitz and I. Stegun, *Handbook of Mathematical Functions.* New York: Dover, 1972.

Leonardo R. A. X. de Menezes (S'89–M'91) was born in Brasilia, Brazil, in 1966. He received the degree in electrical engineering in 1990 and the M.Sc. degree in 1993, both from the University of Brasilia (UnB). He is the recipient of a scholarship of the Government of Brazil, and has recently completed the Ph.D. degree in electrical engineering at the University of Victoria, Victoria B.C., Canada.

His research involved TLM modeling of general media and accuracy of TLM and FDTD methods. His interests are in the areas of numerical modeling, (RF) radio frequency components and systems, semiconductor devices, and electromagnetic theory. He is now interested in inverse problems.

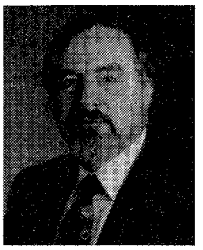

Wolfgang J. R. Hoefer (F'91) received the Dipl.-Ing. degree in electrical engineering from the Technische Hochschule Aachen, Germany, in 1965, and the D.Ing. degree from the University of Grenoble, France, in 1968.

During the academic year 1968 and 1969 he was a Lecturer at the Institut Universitaire de Technologie de Grenoble and a Research Fellow at the Institut National Polytechnique de Grenoble, France. In 1969 he joined the Department of Electrical Engineering, the University of Ottawa, Canada where he was a Professor until March 1992. Since April 1992 he has held the NSERC/MPR Teltech Industrial Research Chair in RF Engineering in the Department of Electrical and Computer Engineering, the University of Victoria, Canada, and he is a Fellow of the Advanced Systems Institute of British Columbia. During sabbatical leaves he spent six months with the Space Division of AEG-Telefunken in Backnang, Germany (now ATN), and six months with the Electromagnetics Laboratory of the Institut National Polytechnique de Grenoble, France, in 1976/77. During 1984 and 1985 he has been a Visiting Scientist at the Space Electronics Directorate of the Communications Research Centre in Ottawa, Canada. He spent a third sabbatical year in 1990 and 1991 as a Visiting Professor at the Universities of Rome "Tor Vergata" in Italy, Nice, Sophia Antipolis in France, and Munich (TUM) in Germany. His research interests include numerical techniques for modelling electromagnetic fields and waves, computer-aided design of microwave and millimeter wave circuits, microwave measurement techniques, and engineering education. He is the Co-Founder and Managing Editor of the *International Journal of Numerical Modelling*.